Inflammation Research (2019) 68:691–704
https://doi.org/10.1007/s00011-019-01252-w

Inflammation Research

ORIGINAL RESEARCH PAPER

Protective effect of galangin against dextran sulfate sodium (DSS)-induced ulcerative colitis in Balb/c mice

Rajendra Sangaraju[1,2] · Nasiruddin Nalban[1,2] · Sateesh Alavala[1] · Vinoth Rajendran[1] · Mahesh Kumar Jerald[3] · Ramakrishna Sistla[1,2]

Received: 6 March 2019 / Revised: 16 May 2019 / Accepted: 24 May 2019 / Published online: 30 May 2019

Abstract

Objective and design Inflammatory bowel disease (IBD) is known to cause chronic inflammation in the digestive tract by the immune malfunction. Herein, we demonstrate the protective effect of galangin (GAL), a phytochemical, on LPS-induced inflammation in cultured mouse macrophages (RAW 264.7) and the treatment of DSS-induced ulcerative colitis in Balb/c mice. However, the anti-inflammatory effect of GAL in DSS-exposed experimental colitis has not been investigated.

Materials and methods We determined the levels of proinflammatory cytokines by ELISA, biochemical analysis using standard protocols and protein expression level of NF-κB signaling pathway and activation of Nrf2 gene pathway were analyzed by western blot analysis in colitis-induced mice.

Results Our in vitro studies showed that LPS-stimulated RAW 264.7 cells treated with GAL reduced the levels of nitrites, IL-6, and TNF-α in a concentration-dependent manner. The results demonstrated that oral administration of GAL at 20 mg/kg (lower dose) and 40 mg/kg (higher dose) significantly reduced the severity of colitis and mitigated the clinical signs of both macroscopic and microscopic of the disease. The levels of proinflammatory cytokines (TNF-α and IL-6) in colonic tissue and serum were reduced significantly and in GAL + DSS-treated group relative to DSS alone treated group. Increased levels of anti-inflammatory cytokine (IL-10) was detected in colon tissues in GAL + DSS-treated groups relative to DSS alone treated group. We also observed decreased levels of myeloperoxidase (MPO), nitrites and TBARS with increased SOD in colonic tissue of GAL + DSS group. Besides, GAL + DSS-treated animals significantly suppressed protein expressions of p-NF-κB and p-Ikk-βα, COX-2, iNOS, Nrf2 and increased HO-1 levels in colon tissues by inhibiting inflammation and oxidative stress.

Conclusion Our study highlights the protective effect of galangin as an anti-inflammatory agent against the severe form of colitis in pre-clinical models suggesting its potency for the treatment of IBD in humans.

Keywords Galangin · Ulcerative colitis · Inflammation · NF-κB pathway · Dextran sulfate sodium

Abbreviations

ANOVA	Analysis of variance
BCA	Bicinchoninic acid
BSA	Bovine serum albumin
CD	Crohn's disease
CDNB	1-Chloro-2,4-dinitrobenzene
COX-2	Cycloxygenase-2
DSS	Dextran sulfate sodium
DTNB	Dithiobis-nitrobenzoic acid
GAL	Galangin
GIT	Gastrointestinal disorder
GSH	Reduced glutathione
GSSG	Oxidized glutathione
GST	Glutathione-S-transferase
HO-1	Heme oxygenase1
H&E	Hematoxylin and eosin staining
IκB	Inhibitor of kappa B
IL-6	Interleukin 6
IL-10	Interleukin 10
IBD	Inflammatory bowel disease

Responsible Editor: John Di Battista.

✉ Ramakrishna Sistla
sistla@iict.res.in

[1] Department of Applied Biology, CSIR-Indian Institute of Chemical Technology (IICT), Hyderabad 500 007, India

[2] Academy of Scientific and Innovative Research (AcSIR), CSIR-HRDC Campus, Sector 19, Kamla Nehru Nagar, Ghaziabad, Uttar Pradesh 201 002, India

[3] Animal House Facility, CSIR-Centre for Cellular and Molecular Biology (CCMB), Hyderabad 500 007, India

iNOS	Inducible nitric oxide synthase
LPS	Lipopolysaccharide
MDA	Malondialdehyde
MTT	3(4,5-Dimethylthiazol-2-yl)-2,5-diphenyltetrazolium bromide
NFκB	Nuclear factor-κB
Nrf2	Nuclear factor erythroid 2-related factor 2
RIPA	Radioimmunoprecipitation assay
ROS	Reactive oxygen species
RNS	Reactive nitrogen species
SEM	Standard error of the mean
SOD	Superoxide dismutase
TBARS	Thiobarbituric acid reactive substances
TLR-4	Toll-like receptor 4
TNF-α	Tumor necrosis factor-α
UC	Ulcerative colitis

Introduction

Inflammatory bowel disease (IBD) is characterized by an imbalance in proinflammatory and anti-inflammatory reactivity leading to oxidative stress of gastrointestinal epithelial cells and alterations in gut microbiota [1–3]. The incidence of IBD is estimated to be dramatically increased in most developing countries affecting millions of people, which requires long-term medical care [4]. Ulcerative colitis (UC) causes chronic inflammation by altering the distal rectal colon and continues into large intestine of colonic mucosa and submucosa [5]. The current pharmacological interventions such as salicylates, immunomodulators, glucocorticoids and anti-TNF agents [6] used in treating UC patients display moderate curative effects [7, 8]. Identifying a new class of therapeutic agents exhibiting undesirable toxic effects could result in greater efficacy on UC pathogenesis. However, the interplay between microbial, environmental and genetical factors resulted in the dysregulation of the mucosal immune system [9]. As a result, the production of proinflammatory cytokines, nitric oxide production through activation of NF-κB signaling leads to a severe form of colitis and its association with carcinogenesis [10].

Moreover, activated neutrophils release reactive oxygen metabolites and trigger the intestinal inflammation causing colon tissue injury [11]. Nonetheless, suppressing the inflammatory signaling mediators and activation of antioxidant enzymes could be a viable strategy to alleviate UC-induced pathogenesis. In the current study, dextran sodium sulfate (DSS) is used as colitis-inducing agent in a mouse model which resembles human colitis and a robust system to screen potential therapeutic agents [12, 13].

Galangin (GAL) a phenolic phytochemical isolated from *Propolis* and *Alpinia officinarum,* used in traditional medicine for various ailments [14]. Considerable evidence shows that galangin possess diverse therapeutic potential against a variety of diseases such as anticancer [15, 16], anti-inflammatory [17], anti-arthritic [18], anti-obesity [19], antioxidant [20] properties. A study shows that galangin protects acetaminophen overdosed, acute liver injury and acute kidney injury in mice [21]. Galangin protected cisplatin-induced nephrotoxicity by inhibiting ERK and NF-κB signaling or MAPK signaling in mice [22, 23]. Also, galangin impedes LPS-induced acute lung injury in collagen-induced arthritis by suppressing NF-κB in mice [24, 25]. However, the protective role of galangin on DSS-induced ulcerative colitis has not been well studied. Therefore, we aim to evaluate the underlying molecular actions of galangin in LPS-induced macrophage cells in culture and DSS-induced ulcerative colitis in the mouse model.

Materials and methods

Chemicals, kits and antibodies

Galangin (purity: ≥ 98%) from Sigma Aldrich, USA, lipopolysaccharide (LPS), (*Escherichia coli* 055: B5), 3-(4, 5-dimethylthiazole-2-yl)-2,5-diphenyltetrazolium bromide (MTT), Griess reagent, reduced glutathione (GSH), glutathione-S-transferase (GST), malondialdehyde (MDA); 5,5′-dithio-bis (2-nitrobenzoic acid) (DNTB), 2-thiobarbituric acid (TBA), superoxide dismutase (SOD) assay kit, and o-dianisidine were obtained from Sigma-Aldrich Co, St Louis, MO, USA. Dextran sulfate sodium (DSS) (molecular weight 36,000–50,000 was purchased from MP Biomedicals, Solon, OH, USA) and sulphanilamide was purchased from Loba chemie Pvt Ltd Mumbai. *N*-(1-Naphthyl)-ethylenediamine dichloride (NED) was obtained from S.D Fine Chem Ltd. Mumbai, India. Polyvinylidene difluoride membranes (PVDF), Radioimmunoprecipitation (RIPA) buffer, Halt protease inhibitor cocktail, NE-PER nuclear and cytoplasmic extraction kit and Bicinchoninic acid (BCA) protein assay kits were obtained from Pierce Biotechnology, Rockford, IL, USA. RPMI 1640, DMEM culture medium and fetal bovine serum (FBS) were obtained from Invitrogen-Gibco (Grand Island, NY, USA). Mouse-specific TNF-α and IL-6 ELISA kits were obtained from BD Opt EIA, BD Biosciences, San Diego, CA, USA and mouse-specific IL-10 was obtained from R&D Systems Bio-Techne, Minnesota, USA. NF-κB(p65) transcription factor assay kit was obtained from Cayman Chemical Company, Ann Arbor, MI, Antibodies against NF-κB(p65), p-IκBα, IκBα, Nrf2, HO-1, iNOS COX2, β-actin, lamin B and horseradish peroxidase (HRP)-conjugated secondary antibody were purchased from Cell Signaling Technology (Boston, MA), Enhanced Chemiluminescent detection reagents substrate (Supersignal West

Pico, Pierce Biotechnology, Rockford, IL, USA). All other chemicals were analytical grade products.

Cell viability assay

Cell viability was determined using the MTT reduction assay. RAW 264.7 cells were cultured in RPMI-1640 media containing 10% fetal bovine serum (FBS) and 1% antibiotic–antimycotic mix and seeded into 96-well plate at a density of 10,000 cells/well. Different concentrations of galangin (0–25 µg/mL) were treated in the presence or absence of LPS (100 ng/mL) for 24 h. After 24 h incubation, 10 µL of MTT solution (5 mg/mL in PBS) was incubated for an additional 4 h at 37 °C and 100 µl of dimethyl sulfoxide was added to solubilize the formazan crystals formation. The optical density was read at 570 nm using a microplate reader (BioTech Synergy 4, USA).

Determination of proinflammatory cytokines and nitrite levels in cultured macrophage cells (RAW264.7)

RAW264.7 cells were seeded and pre-treated with galangin at two different concentrations 0.39 µg/mL and 0.78 µg/mL for 1 h, followed by LPS stimulation for next 18 h at 37 °C. After 18 h of incubation, the culture supernatant was collected and analyzed for levels of proinflammatory cytokines (TNF-α and IL-6) using ELISA kits and measured at an optical density of 450 nm. The nitrite levels were measured by Griess reagent, and the nitrite concentration was determined using sodium nitrite as a standard [26].

Animal studies

All animal experiments were performed in healthy male Balb/c mice (4–5 weeks old, weighing 24–28 g) which were acclimatized to the laboratory conditions for about 7 days before initiation of the study in the BIOSAFE, an animal quarantine facility of CSIR-Indian Institute of Chemical Technology (IICT), Hyderabad, India (Registration No: 97/GO/RBi/S/1999/CPCSEA). Mice were allowed free access to standard pellet diet and fresh drinking water ad libitum. They were housed under standard laboratory conditions with 12 h/12 h of light/dark cycle, 22 ± 2 °C and 40–70% RH throughout the study protocol. The protocols for animal use were approved by the CSIR-IICT, Institutional Animal Ethics Committee (IAEC) and all experiments were performed in accordance with the guidelines for safe use and care of experimental animals by Committee for the Purpose of Control and Supervision of Experiments on Animals (CPCSEA) Government of India (Approval no: IICT/63/2016).

Induction of ulcerative colitis by DSS and treatment regimen in mice

DSS-induced experimental colitis model was developed by oral administration of 4% (w/v) DSS in drinking water for 5 consecutive days (days 8–12). For comparison, the vehicle control group was treated with DSS-free drinking water. The dosages of galangin were selected based on previous reports [24, 27, 28]. Galangin was administered through oral delivery suspended in 2% gum acacia at two different dosages 20 or 40 mg/kg of body weight. Both the dosages were given to animals from day 0 to 12. Randomly, the mice were divided into five groups consisting of six animals in each group ($n = 6$). Group I: vehicle control (2% gum acacia without GAL), Group II: Test drug-Galangin 40 mg/kg (without DSS), Group III: DSS control, Group IV: DSS + GAL (20 mg/kg BW, low dose), Group V: DSS + GAL (40 mg/kg BW, high dose).

On day 12, the serum was collected aseptically and the animals were euthanized under CO_2 asphyxiation and the colon tissue was dissected and measured for colon length. A portion of the colon tissue was stored in 10% buffered formalin for histopathological analysis at room temperature and the remaining colon tissue was stored at − 80 °C for further biochemical and immunoblot analysis. All the estimate parameters in the study were obtained from the distal colon tissues (Fig. 2a).

Assessment of disease activity index (DAI)

Animals were examined daily from day 8 to 12 (i.e., during DSS treatment) for change in net body weight and the disease activity index (DAI). At the end of the intervention (i.e. on day 12), disease activity index was determined by the sum of scores given as for: body weight loss (scored as: 0, none; 1, 1–5%; 2, 5–10%; 3, 10–20%; 4, > 20%), stool consistency (scored as 0, well-formed pellets; 2, loose stools; 4, diarrhea) and the presence or absence of fecal blood (scored as 0, negative hemoccult test; 2, positive hemoccult test; 4, gross bleeding). The colon tissue was dissected and colons were measured for colon length and examined for gross macroscopic appearance and stool consistency in tissues.

Histopathological evaluation

Colon tissues were excised from all the experimental groups on day 12, fixed in 10% phosphate-buffered formalin, processed and embedded in paraffin and sectioned to approximately 5 µm thickness using a microtome (Leica, Bensheim, Germany), and stained with hematoxylin and eosin (H&E) for pathological evaluation. The sections were then evaluated for histological changes under light microscopy, and the images were taken using the 400× objective (Axiovision software,

Axioplan 2 Imaging, Zeiss microscope). Histological examination was performed by an investigator with no knowledge of the experimental groups.

Myeloperoxidase (MPO) activity assay

MPO activity indicates a measure of neutrophil infiltration of ulcerative colitis. Colon tissues were homogenized in ice-cold 0.1 M potassium phosphate buffer (pH 6.5) containing 0.5% hexadecyltrimethylammonium bromide (HTAB) and 10 mM EDTA. The obtained tissue homogenates were centrifuged at 13,100×*g* for 20 min at 4 °C. The aliquot of the supernatant (0.1 mL) was mixed with 2.9 mL of 50 mM phosphate buffer containing 0.167 mg of o-dianisidine hydrochloride and 0.0005% hydrogen peroxide. The change in absorbance over 5 min was measured at 460 nm. The results were expressed as U/g of tissue [29].

Assay of colon tissue antioxidant status

The colon tissue homogenate was prepared as described [30]. The obtained supernatant of colon tissue was used for the estimation of various antioxidants, such as reduced glutathione (GSH), glutathione-S-transferase (GST) and superoxide dismutase (SOD) and nitrite levels. The pellet obtained was mixed with 10% trichloroacetic acid, re-suspended and centrifuged at 1800*g* for 10 min. The obtained supernatant was used for the estimation of thiobarbituric acid reactive substance (TBARS) contents. The total protein content was estimated using Bicinchoninic acid (BCA) assay kit (Pierce Biotechnology, Rockford, IL, USA) against BSA as standard.

The reduced glutathione (GSH) content in colon tissue was determined according to the method of Ellman's by reacting with DTNB. The level of GSH was determined from GSH (Sigma-Aldrich) standard curve and the results were expressed as mg of GSH/g of tissue.

Briefly, 20 µL of the tissue supernatant was added to an equal volume of GSH and 150 µL of potassium phosphate buffer (0.1 M, pH − 6.5). To this mixture, 10 µL of CDNB was added and the rate of change of absorbance of CDNB with time at 340 nm was studied for 5 min at 1 min interval using the kinetic program in the microplate reader. The activity was expressed as nmol of CDNB conjugated/min/mL. The molar extinction coefficient of CDNB is 0.00503/µM The SOD activity of colonic tissue was measured using superoxide dismutase assay kit as per manufacturer specifications.

Estimation of lipid peroxidation and nitrites of colonic tissues

The supernatant obtained from the 10% TCA fraction was allowed to react with thiobarbituric acid (0.067% in distilled water). The amount of TBARS formed was measured at 523 nm as nmol of malondialdehyde eq/g of tissue. The amount of nitrites, as an index of nitric oxide was determined by reaction with Griess reagent and interpolated from sodium nitrite standard curve and the absorbance of the resulting azo compound was measured at 540 nm. The results were expressed as µM/g of tissue.

Determination of inflammatory cytokines

Serum and colon tissue of around 60 mg from each animal was weighed, minced and a 10% tissue homogenate was prepared in ice-cold phosphate buffer saline (PBS, pH 7.4) containing 1% Halt protease inhibitor cocktail. The homogenate was centrifuged at 5000*g* for 20 min at 4 °C and the supernatant was used for the estimation of TNF-α and IL-6 levels using mouse-specific TNF-α and IL-6 using the ELISA respective kits (BD Opt EIA, BD Biosciences, San Diego, CA, USA) as per manufacturer instructions and also the supernatant was estimated for anti-inflammatory cytokine IL-10 using mouse-specific IL-10 using ELISA according to the procedure recommended by the supplier (R&D SYSTEMS Bio-Techne, Minnesota, United States). The total protein content in the supernatant was estimated using BCA protein assay kit (Pierce Biotechnology, Rockford, IL, USA) against bovine serum albumin (BSA) as standard. The concentrations of all cytokines were expressed as pg/g of protein.

Western blot analysis

Briefly, colon tissues from different experimental groups were homogenized in Radioimmunoprecipitation (RIPA) lysis buffer (Pierce Biotechnology, Rockford, IL, USA) containing 1% Halt protease inhibitor cocktail to obtain whole-tissue extracts. Similarly, the extracts of nuclear and cytoplasmic contents were prepared using NE-PER nuclear and cytoplasmic extraction kit (Pierce Biotechnology, Rockford, IL, USA) as described in manufacturer instructions. The supernatants collected were determined using a Bradford reagent and equivalent amounts of protein were resolved by SDS-PAGE analysis and transferred onto polyvinylidene difluoride (PVDF) membrane (Pierce Biotechnology, Rockford, IL, USA). Membranes were blocked in 3% BSA for 1 h and then incubated at 4 °C for overnight with specific primary antibodies. All the primary and secondary antibodies were obtained from Cell Signaling Technology and used at recommended dilutions. The expressions of NF-κB (p65) (1:500), phospho-IκBα (1:1000), IκBα (1:1000), COX-2 (1:1000), iNOS (1:1000), HO-1 (1:1000) and Nrf2 (1:1000) were studied. β-actin (1:1000) was used as housekeeping protein for whole-tissue extracts and lamin B (1:1000) was used as housekeeping protein for nuclear extracts. The blots

were visualized using chemiluminescence detection reagents (Supersignal West Pico Pierce Biotechnology, Rockford, IL, USA) and Vilber-Fusion-Western blot Chemiluminescence Imaging system. The densitometry analysis of each blot was performed using Image J software NIH, USA.

Statistical analyses

All statistical analyses were performed using one-way ANOVA with GraphPad Prism, version 5.0 software. Comparisons between groups were performed by applying post hoc Dunnett's multiple comparison procedures with reference to the DSS control group. Results were expressed as mean ± standard error of the mean (SEM). Statistical significance was considered when the p value was less than 0.05.

Results

Effect of galangin on LPS-stimulated mouse macrophage cells in culture

The effect of galangin on the growth of RAW 264.7 macrophage was examined by MTT assay for 24 h, with varying concentration (Fig. 1a). The treated cells did not show any cytotoxic effects up to 1.56 µg/mL. Therefore, to assess the anti-inflammatory activity of galangin two different concentrations of 0.39 and 0.78 µg/mL was tested in the presence of LPS (100 ng/mL). The levels of nitrites, IL-6, TNF-α, were determined in the culture supernatant (Fig. 1c–e). There was a significant decrease in nitrites, IL-6, TNF-α ($p < 0.001$) in comparison to their counterparts. These results demonstrate that treatment with galangin markedly reduced the levels of proinflammatory cytokines and nitrite content when stimulated with LPS suggesting the role of galangin as an anti-inflammatory agent.

Effect of galangin on symptoms of DSS-induced colitis in mice

The dose-dependent effect of galangin was evaluated on DSS-exposed mice. We assessed the colitis severity score (DAI, disease activity index) such as weight loss, stool consistency and stool blood as a measure of disease severity on day 12. It was observed that DSS alone treated mice showed severe disease progression of acute colitis with DAI score of 2.55 ± 0.23. On the other hand, galangin-treated group at 20 and 40 mg/kg body weight showed reduced DAI scores 1.83 ± 0.20 at 20 mg/kg and 1.00 ± 0.05 at 40 mg/kg, respectively (Fig. 2b). Furthermore, mice treated with DSS alone showed body weight loss, shortening of colons whereas, galangin-treated mice retained weight loss and colon length shortening (Fig. 2c–e). Thus, galangin exhibited a curative effect on DAI score, net body weight, and colon length against DSS-induced ulcerative colitis in mice.

Effect of galangin on colon histology of DSS-induced mice

We assessed the severity of distal colon tissue damage by histopathological analysis using Hematoxylin and Eosin (H and E) staining. It was observed that distal colons from vehicle control (without DSS) and galangin 40 mg/kg (without DSS) treated mice showed normal mucosal epithelial cells along with submucosal glands with no observable ulceration or inflammation. Colon tissue of DSS alone treated group showed the destruction of crypt structure with loss of goblet cells, disruption of the epithelial layer, moderate to severe submucosal inflammation along with infiltration of inflammatory cells, massive infiltration of inflammatory cells with cryptic abscess compared to colon tissue without DSS. Noticeably, colon tissue of DSS + GAL treatment showed a dose-dependency reduction on the histology of colon tissue damages. Galangin-treated group exhibited minimal cryptic damage with preserved goblet cells and epithelial lining, mild submucosal hemorrhages along with mild foci of infiltration of inflammatory cells in the sub mucosal region in colon tissue. Therefore, our results show that treatment with galangin effectively reduced the signs of inflammation and retained the structural integrity with minimal pathological damage in colon tissue (Fig. 3a–e).

Effect of galangin on myeloperoxidase (MPO) activity in colon tissue of DSS-induced mice

The results showed that MPO activity in the DSS alone treated group, an index of neutrophil infiltration, was significantly ($p < 0.001$) increased when compared with the vehicle control (without DSS). Treatment with DSS + GAL at 20 and 40 mg/kg, the MPO activity ($p < 0.01$ at 20 mg/kg and $p < 0.001$ at 40 mg/kg) significantly decreased with increase in dose as compared to DSS alone treated group (Fig. 3f).

Effect of galangin on oxidative stress markers in colon tissue of DSS-induced mice

Next, we determined the impact of galangin in understanding the role of oxidative stress markers in colitis. Treatment with DSS alone significantly decreased the levels of GST, GSH and SOD and increased the nitrite and TBARS ($p < 0.001$) versus the vehicle control group. In contrast, DSS + GAL at 20 and 40 mg/kg restored the levels of GST, GSH and SOD with decreased levels of nitrite and TBARS relative to DSS control group. Therefore, our results show that galangin improved the levels of oxidative stress markers in colonic tissue (Fig. 4a–e).

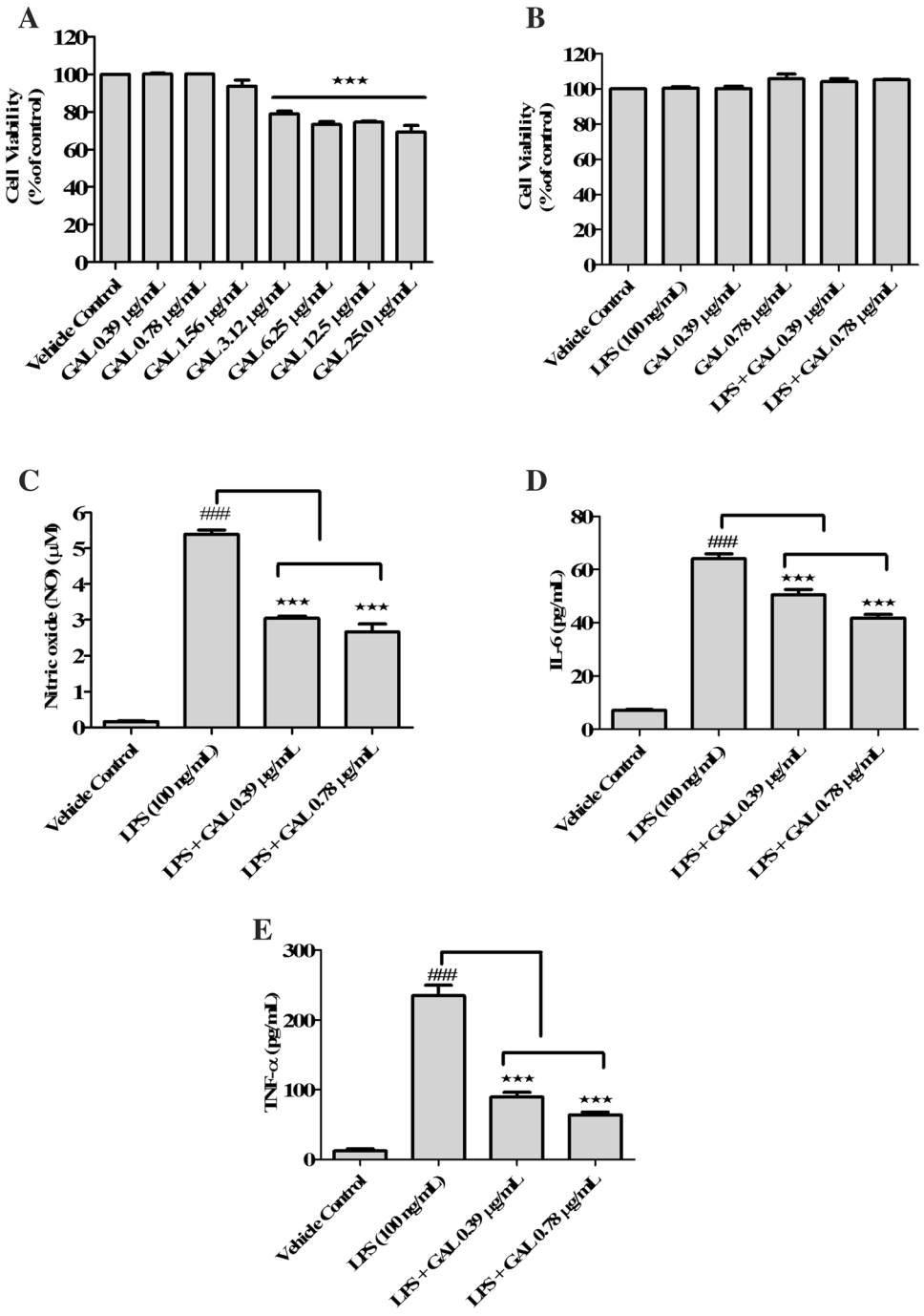

Fig. 1 Effect of galangin on LPS-treated murine macrophage cells in culture. **a**, **b** The cells were treated with galangin at different doses in the absence or presence of LPS on the viability of mouse macrophages RAW 264.7 using MTT assay. ***$p < 0.001$ were compared with the control cells (no treatment). In vitro anti-inflammatory effect of galangin in the presence of LPS on mouse macrophages on the levels of **c** nitrites, **d** interleukin-6 (IL-6) and **e** tumor necrosis factor-α (TNF- α) after 18 h post-treatment. Data are expressed as the mean ± SEM of three independent experiments. ###$p < 0.001$ was compared with the control cells (no treatment); ***$p < 0.001$ was compared with the LPS alone treated cells

Effect of galangin on cytokine levels in colon and serum of DSS-induced mice

To study the immunosuppressive role of galangin on the production of proinflammatory cytokines (TNF-α and IL-6), colon tissue and serum was collected on day 12. We observed increased levels of TNF-α and IL-6 in DSS alone treated group whereas the vehicle control group showed negligible levels. Treatment with DSS + GAL at 20 and 40 mg/kg significantly ($p < 0.001$) reduced the cytokine levels in colon tissue and serum in comparison to DSS alone treated group. Thus, administration of galangin at both doses exhibited a dose-dependent reduction on the production of TNF-α and IL-6 in both colon tissue and serum. We also observed that anti-inflammatory cytokines (IL-10) levels were significantly ($p < 0.001$) increased in the DSS + GAL-treated group at 20 and 40 mg/kg compared to the DSS alone treated group (Fig. 5e). Therefore, galangin exerts its protective effect by regulating the expression levels of both pro- and anti-inflammatory cytokines.

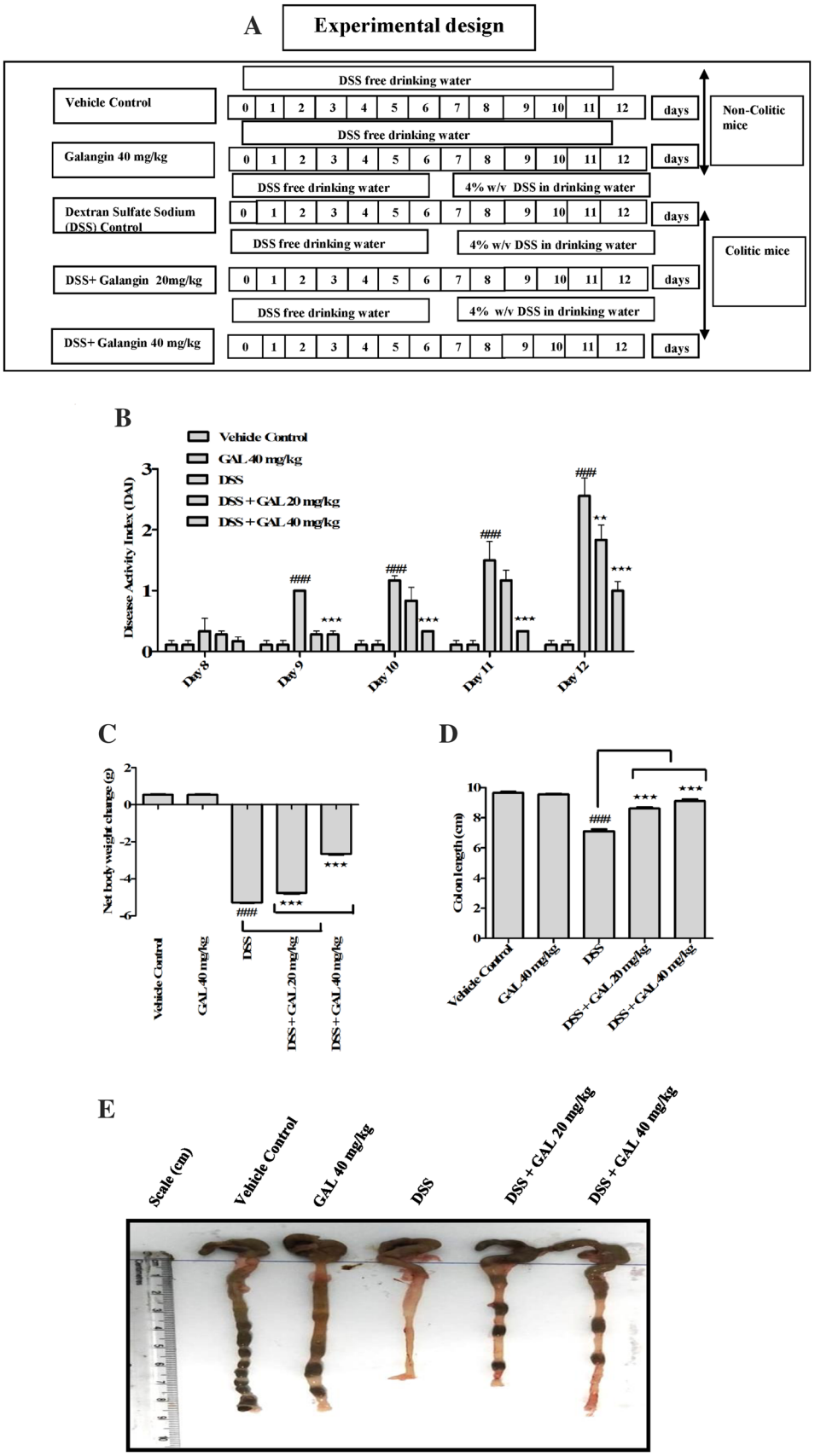

Fig. 2 Effect of galangin on the clinical symptoms in colon tissue of DSS-induced mice. Ulcerative colitis was induced in Balb/c mice by administering 4% DSS in the drinking water for 5 days (day 8–12) and treated with galangin from day 0 to 12. **a** Schematic representation on the experimental design. **b** Disease Activity Index scores in colonic mice. **c** Net body weight change was measured during DSS treatment. **d** Colons was harvested on day 12 and the changes in colon length were measured. **e** Representative images of the colon showing the disease severity between DSS alone treated versus DSS + GAL-treated group. Data are presented as the mean ± SEM ($n = 6$). $^{###}p < 0.001$ vs vehicle control; $^{*}p < 0.05$, $^{**}p < 0.01$, $^{***}p < 0.001$ vs DSS alone

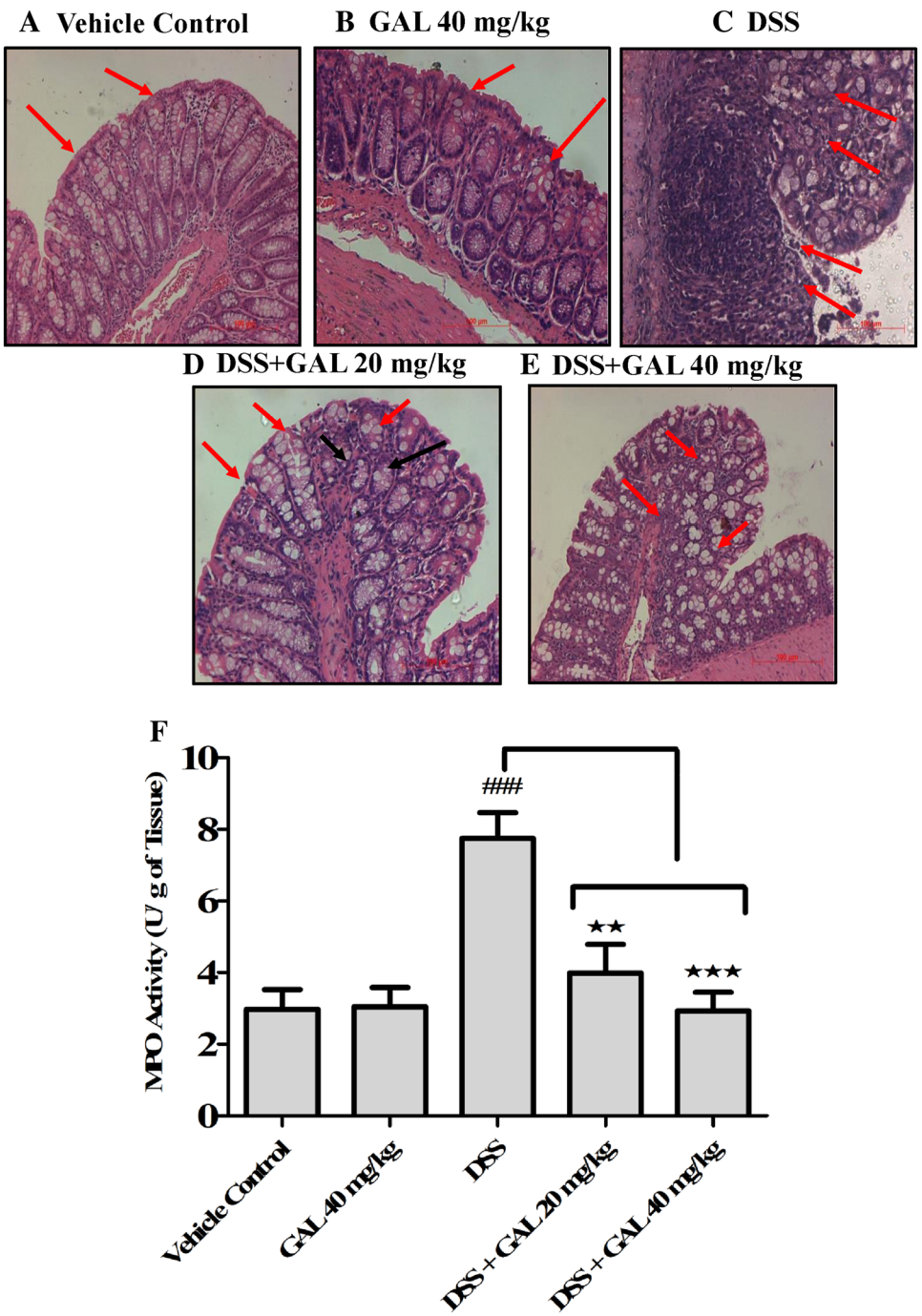

Fig. 3 Effect of galangin treatment on histopathological injury in DSS-induced colitis. Representative photomicrograph of colonic tissue stained with hematoxylin and eosin of all experimental groups. **a** Vehicle control (without DSS and GAL): normal mucosal epithelial cells along with submucosal glands with no ulceration or inflammation were observed. **b** Galangin treatment at 40 mg/kg (without DSS) displayed similar morphology to vehicle control: **c** DSS alone treated mice: moderate to severe submucosal inflammation along with infiltration of inflammatory cells indicated in arrow **d** GAL (20 mg/kg) + DSS: mild submucosal hemorrhages [red arrow] along with mild foci of infiltration of inflammatory cells were observed in submucosal region [black arrow]. **e** GAL 40 mg/kg + DSS: mucosal epithelial cells are normal and no ulceration or inflammation with mild sub mucosal infiltration of inflammatory cells was observed [arrow]. **f** Myeloperoxidase activity (MPO) activity in colon tissue. Data are expressed as mean ± SEM. $^{###}p < 0.001$ vs control, $^{**}p < 0.01$ $^{***}p < 0.001$ vs DSS alone (color figure online)

Effect of galangin on downstream targets of NF-κB signaling in colon tissue of DSS-induced mice

The effect of galangin on the expression of downstream targets of NF-κB signaling pathway was studied in colon tissue. The colon tissue of DSS-induced mice significantly increased the expression of p-NF-κB and p-Ikk-β/α ($p < 0.001$) as relative to vehicle control mice on day 12. Galangin-treated mice at both the doses (20 and 40 mg/kg) significantly ($p < 0.001$) increased the expression level of phosphorylation of IκBα in the cytoplasmic fraction ($p < 0.001$) and decreased the accumulation of ($p < 0.001$) nuclear NF-κB (p65) ($p < 0.001$) compared to DSS-induced mice. Additionally, we studied the expression of iNOS and COX-2 of NF-κB signaling pathway in response to DSS stimuli in colon tissues. DSS-treated group showed a significant increase in the levels of iNOS and COX-2 versus the vehicle control group. Both the doses significantly reduced ($p < 0.01$ at 20 mg/mg) ($p < 0.001$ at 40 mg/mg) the expression of COX-2 and iNOS compared to DSS alone treated

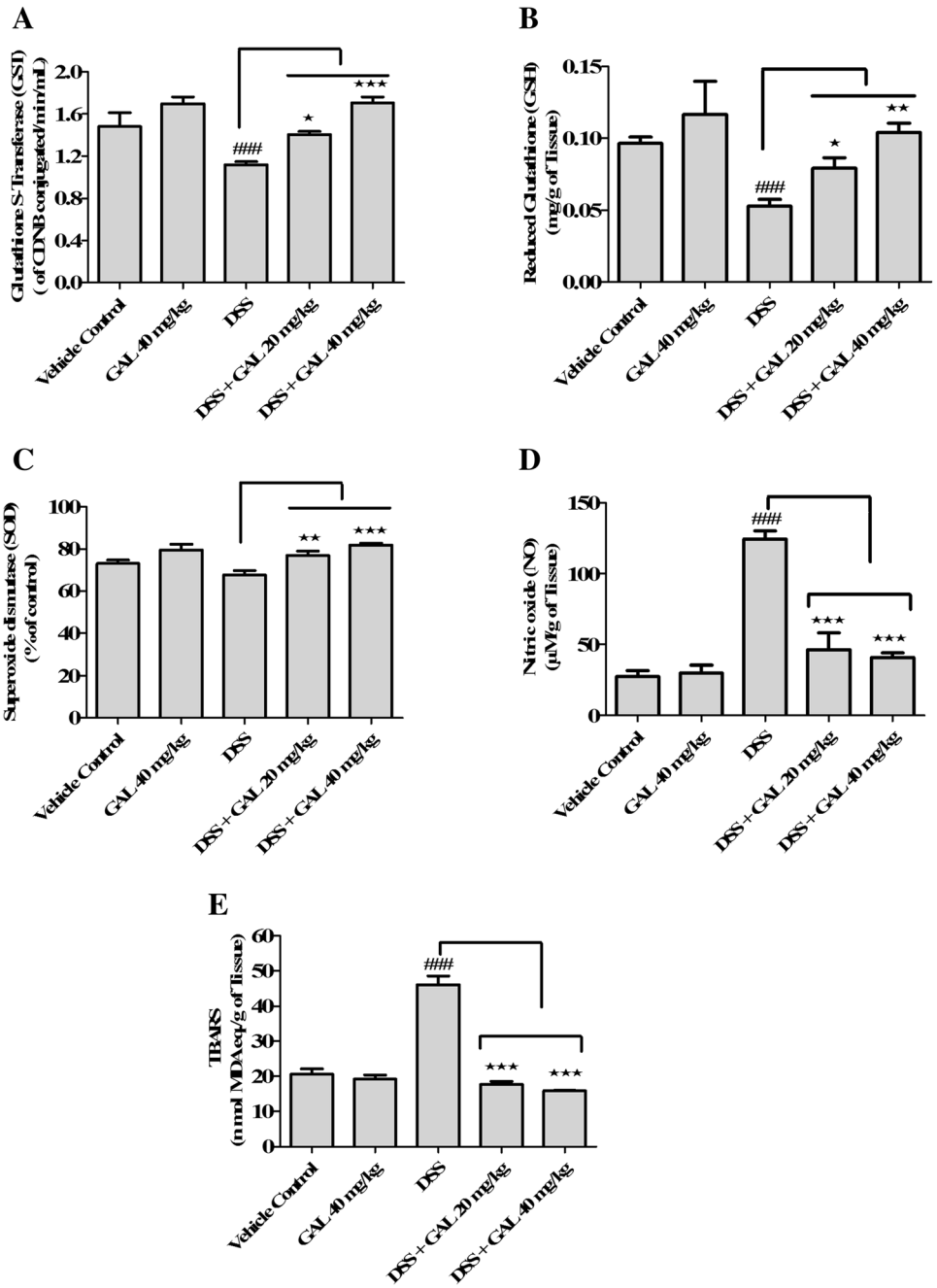

Fig. 4 Effect of galangin treatment on biochemical markers in DSS-induced colonic tissue **a** Glutathione-S-transferase (GST) in colon tissue. **b** Reduced glutathione. **c** Superoxide dismutase (SOD) activity in colon tissue. **d** Nitric oxide levels in colon tissue. **e** Thiobarbituric acid levels in colon tissue. Data are expressed as mean ± SEM. $^{###}p < 0.001$ vs vehicle control; $^{*}p < 0.05$, $^{**}p < 0.01$, $^{***}p < 0.001$ vs DSS alone

group. Thus, galangin exerts its inhibitory effect by suppressing NF-κB activation (Fig. 6).

Galangin activates Nrf2 signaling in colon tissues of DSS-induced mice

Galangin treatment improved the antioxidant levels in DSS-induced colon tissues. We next ventured to evaluate the effect of galangin on the Nrf2 signaling pathway by determining the localization of Nrf2 in the nuclear region and HO-1 in the DSS-induced colon tissues by immunoblotting. We observed a decrease ($p < 0.001$) in the nuclear accumulation of Nrf2 in DSS alone in comparison to vehicle control. On the contrary, treatment with DSS + GAL at both doses significantly increased ($p < 0.01$ for 20 mg/kg and $p < 0.001$ for 40 mg/kg) the nuclear accumulation of Nrf2 and increased the expression of HO-1 in dose-dependency manner as compared to DSS alone treated group. Altogether, galangin imparts protection to mice by improving the antioxidant status in DSS-induced mice (Fig. 7).

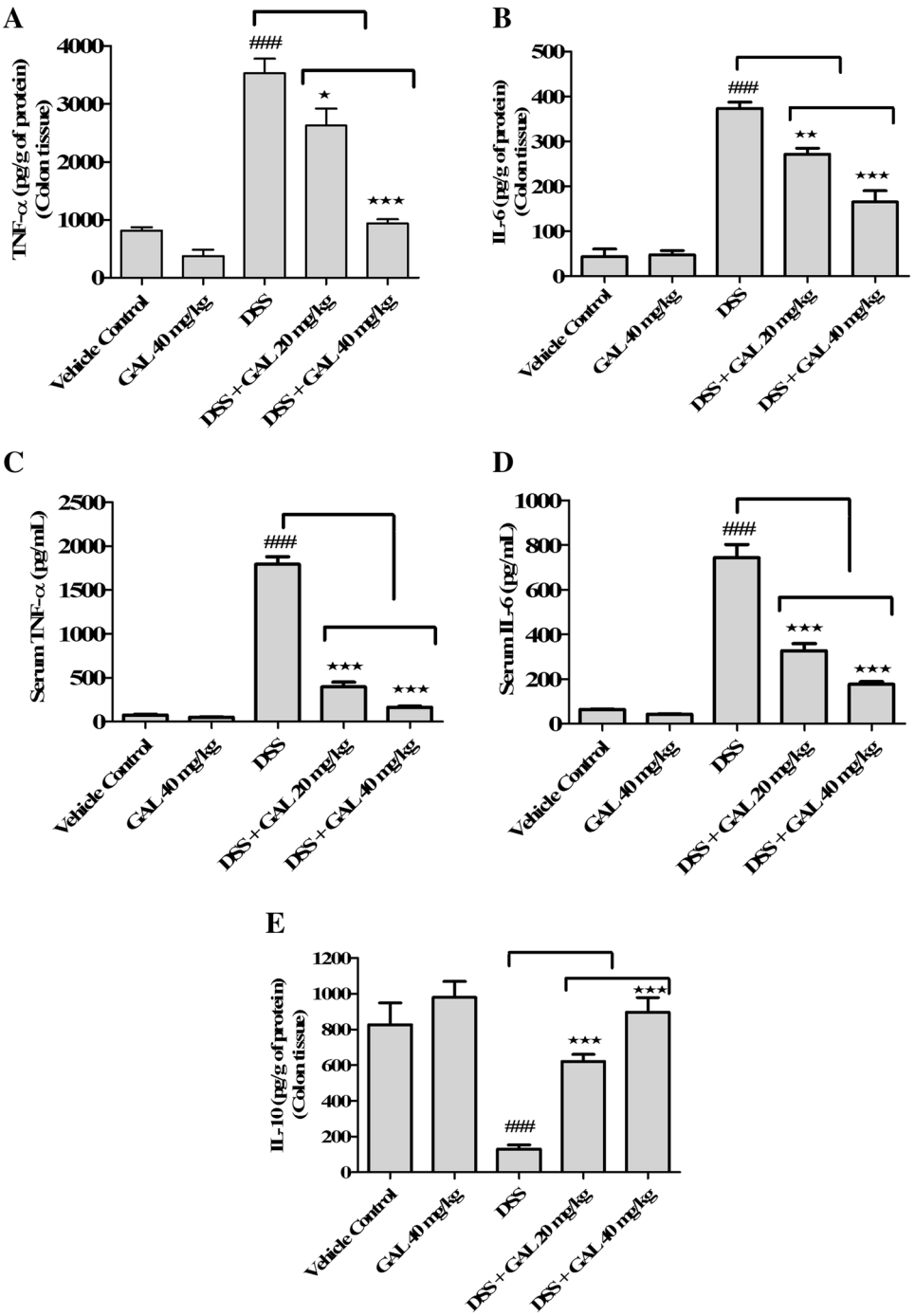

Fig. 5 Effect of galangin on proinflammatory cytokines (TNF-α, IL-6) in DSS-induced colonic tissue and serum. **a**, **b** Proinflammatory cytokines (TNF-α and IL-6) concentration in mouse colonic tissue at day 12 post-treatment of galangin. **c**, **d** TNF- α and IL-6 concentration in mouse serum on day 12 post-treatment of galangin. **e** The levels of anti-inflammatory cytokine IL-10 in colon tissue on day 12 post-treatment of galangin. Cytokines production was quantified by ELISA kits. Data are expressed as mean ± SEM ($n = 6$). $^{###}p < 0.001$ vs vehicle control; $^{*}p < 0.05$, $^{**}p < 0.01$, $^{***}p < 0.001$ vs DSS alone

Discussion

The present findings demonstrated that natural bioflavonoid galangin displayed anti-inflammatory activity in LPS-induced murine macrophage cells in culture and DSS-induced ulcerative colitis in mice model. Accumulating evidence suggests that galangin shows proven therapeutic efficacy against various animal models of inflammation with no apparent toxic effects [31, 32]. However, its protective effect on the intestinal inflammation is not well understood. We evaluated the pharmacological impact of galangin and their mechanism of protection against DSS-induced colitis in mice. We observed that treatment with galangin markedly reduced the levels of TNF-α, IL-6 and nitrite levels under in vitro and in vivo conditions (Figs. 1, 5) Also, treatment with galangin mediated the upregulation of IL-10 in colon tissue corroborated with the previous study that galangin enhanced the level of IL-10 upon LPS

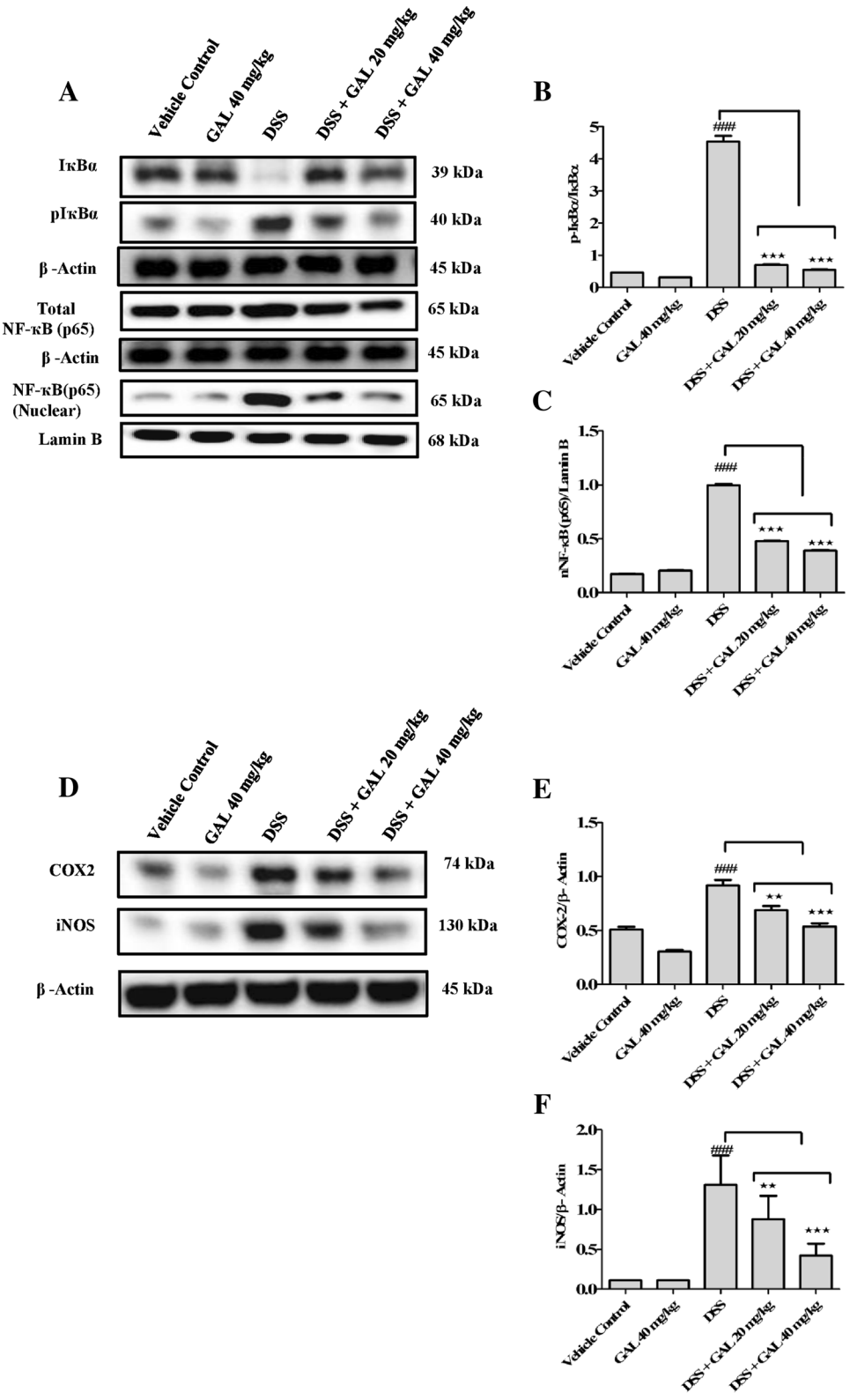

Fig. 6 Effect of galangin treatment on NF-κB signaling pathway in DSS-induced colonic tissue. **a** Representative immunoblot analyses depicting the expression levels of nuclear NF-κB (p65), phospho-IκBα and IκBα expressions in colonic tissue of DSS versus DSS + GAL. **d** Expression levels of COX-2 and iNOS. Lamin B was used as internal control for the nuclear fraction and β-actin was used as internal control for cytoplasmic and total protein fractions. **b**, **c**, **e**, **f** Represents the band intensities quantified using NIH Image J software analysis relative to expression of phospho-IκBα/IκBα ratio, nuclear NF-κB(p65)/lamin B ratio, COX-2/β-actin ratio and iNOS/β-actin. Values are the mean ± SEM ($n = 3$). $^{###}p < 0.001$ vs vehicle control, $^{**}p < 0.01$ and $^{***}p < 0.001$ vs DSS control

stimulation in microglial cells [33, 34]. We also observed that DSS + GAL-treated animals showed improved clinical signs such as reduced body weight loss, retained colon length and reduced the DAI score as shown in Fig. 2. Moreover, galangin prevented the macroscopically visible damage of colon tissues with reduced MPO levels suggesting a reduced accumulation of neutrophils in colon tissues as shown in Fig. 3. These observations indicated that galangin

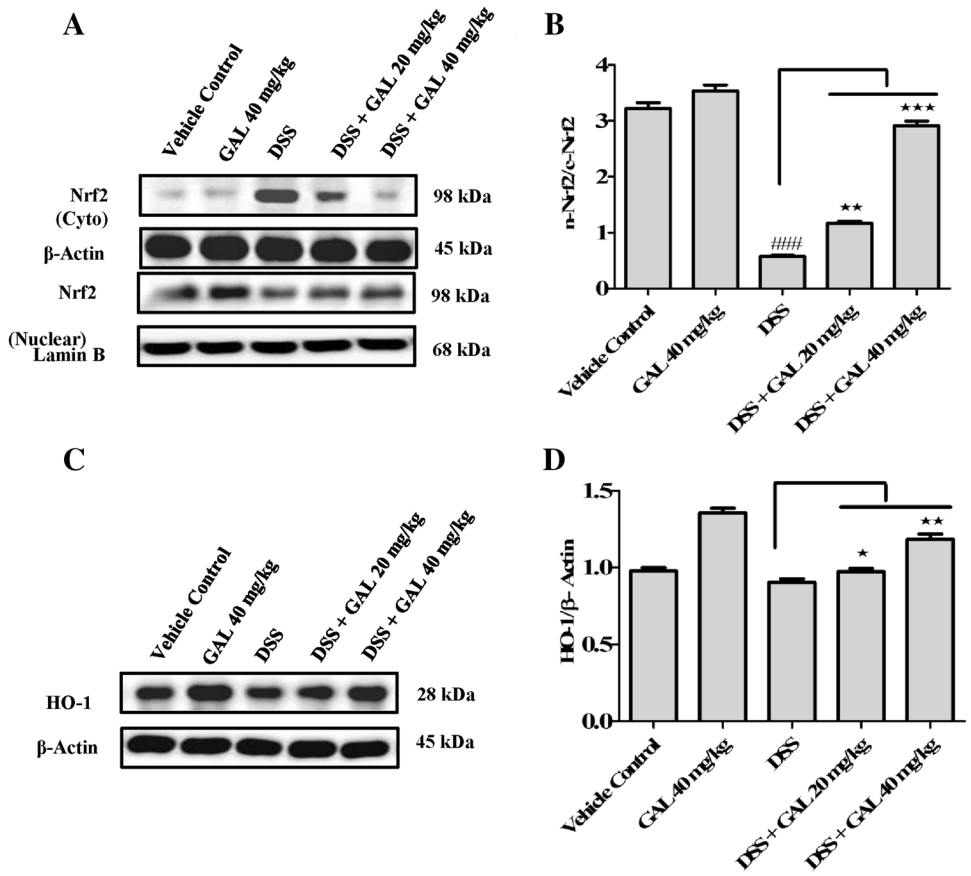

Fig. 7 Effect of galangin treatment on Nrf-2 signaling pathway in DSS-induced colonic tissue. **a**, **c** Representative immunoblot analyses are showing the expression levels of nuclear translocation of Nrf2, HO-1 in colon tissues of DSS versus DSS + GAL. Lamin B was used as internal control for the nuclear fraction and β-actin was used as internal control for cytoplasmic and total protein fractions. **b**, **d** Represents the graphical depiction of band intensities quantified using NIH Image J software analysis relative to expression levels of nuclear Nrf2/cytoplasmic Nrf2 ratio, Total HO-1 proteins. Values are the mean ± SEM ($n = 3$). $^{###}p < 0.001$ vs vehicle control, $^{*}p < 0.05$, $^{**}p < 0.01$ and $^{***}p < 0.001$ vs DSS

attributes protective effect by suppressing proinflammatory markers against DSS-induced colitis.

Furthermore, DSS-treated group displayed severe colon damage due to an increase in the production of free radicals and activation of inflammatory markers. In our findings, DSS + GAL-administered group markedly improved the status of GSH, GST and SOD levels with an increase in TBARS and nitric oxide levels as shown in Fig. 4. Several phytochemicals and their structural analogs imparted greater protection against oxidative stress by activating the Nrf2 pathway in colitis mice [35, 36]. Activation of Nrf2, a basic region-leucine zipper transcription factor, facilitates the upregulation of antioxidant and phase II-detoxifying enzymes by protecting the cells from oxidative damages [37]. An earlier study indicates that Nrf2 activation abolishes the expression of proinflammatory cytokine genes and suppresses the inflammation through redox control [38]. Our investigation revealed that galangin effectively increased the nuclear translocation of Nrf2 by upregulating HO-1 expression (Fig. 7) Thus, galangin confers protection against DSS-induced colitis through Nrf2-mediated antioxidant defensive system. These results corroborate with previous findings that galangin is involved in the activation of ERK/AKT-driven Nrf2 signaling pathway during oxidative stress [39, 40].

It is evident that increased production of inflammatory cytokines causes a severe form of colitis indicating an interplay between Nrf2 and NF-κB pathways [41, 42]. We studied the effect of galangin on pleiotropic transcription factor NF-κB signaling in colon tissues. The previous report suggests that galangin hampered the activation of the NF-κB pathway in LPS-induced cellular and mice models [17, 31]. Our findings indicate that galangin ameliorated DSS-induced colitis by upregulating the antioxidant defenses through Nrf2/HO-1 signaling pathway and inhibited NF-κB signaling pathway. The expression levels of iNOS and COX-2 and phosphorylated IκBα (p-IκBα) proteins were significantly reduced in colitis-induced mice. Reports suggest that the production of proinflammatory cytokines and dysregulation of the mucosal immune system resulted in the disruption of tight junction and intestinal homeostasis in colitis pathogenesis [43, 44]. Notably, there is a strong association between COX-2 and iNOS-induced proinflammatory cytokines at the site of mucosal inflammation in IBD pathogenesis [45, 46]. Therefore, galangin inhibited NF-κB signaling pathway in colitis mice by reducing the expression of proinflammatory cytokines and repressed the translocation of NF-κB as well, disrupted the phosphorylation and degradation of IkB-α with an increase in galangin dosages (Fig. 6).

In summary, oral administration of galangin effectively suppressed the pathogenesis of ulcerative colitis in a mouse model. Together these results suggest the chemo-potential role of dietary component galangin as an anti-inflammatory agent and warrant further studies in clinical use.

Acknowledgements The authors are grateful to Director, CSIR-IICT, Hyderabad, India for providing necessary facilities and continuous support. Rajendra Sangaraju thanks Council for Scientific and Industrial Research (CSIR), New Delhi, India for financial support in the form of Senior Research Fellowship. SA acknowledges the Department of Science and Technology (DST), New Delhi, India for financial assistance in the form of Inspire Fellowship (IF160504) and NN thanks ICMR, New Delhi, India for providing the Senior Research Fellowship. CSIR-IICT Manuscript Communication No: IICT/Pubs/2018/384.

Compliance with ethical standards

Conflict of interest The authors declare no competing financial interest.

References

1. de Mattos BR, Garcia MP, Nogueira JB, Paiatto LN, Albuquerque CG, Souza CL, et al. Inflammatory bowel disease: an overview of immune mechanisms and biological treatments. Mediators Inflamm. 2015;2015:493012.
2. MacDonald TT, Monteleone G, Pender SL. Recent developments in the immunology of inflammatory bowel disease. Scand J Immunol. 2000;51:2–9.
3. Coskun M. Intestinal epithelium in inflammatory bowel disease. Front Med (Lausanne). 2014;1:24.
4. Ng SC, Shi HY, Hamidi N, Underwood FE, Tang W, Benchimol EI, et al. Worldwide incidence and prevalence of inflammatory bowel disease in the 21st century: a systematic review of population-based studies. Lancet. 2018;390:2769–78.
5. Matricon J, Barnich N, Ardid D. Immunopathogenesis of inflammatory bowel disease. Self Nonself. 2010;1:299–309.
6. Raad MA, Chams NH, Sharara AI. New and evolving immunotherapy in inflammatory bowel disease. Inflamm Intest Dis. 2016;1:85–95.
7. Kumar A, Auron M, Aneja A, Mohr F, Jain A, Shen B. Inflammatory bowel disease: perioperative pharmacological considerations. Mayo Clin Proc. 2011;86:748–57.
8. Sales-Campos H, Basso PJ, Alves VB, Fonseca MT, Bonfa G, Nardini V, et al. Classical and recent advances in the treatment of inflammatory bowel diseases. Braz J Med Biol Res. 2015;48:96–107.
9. Kaser A, Zeissig S, Blumberg RS. Genes and environment: how will our concepts on the pathophysiology of IBD develop in the future? Dig Dis. 2010;28:395–405.
10. Viennois E, Chen F, Merlin D. NF-kappaB pathway in colitis-associated cancers. Transl Gastrointest Cancer. 2013;2:21–9.
11. Karin M. NF-kappaB as a critical link between inflammation and cancer. Cold Spring Harb Perspect Biol. 2009;1:a000141.
12. Chassaing B, Aitken JD, Malleshappa M, Vijay-Kumar M. Dextran sulfate sodium (DSS)-induced colitis in mice. Curr Protoc Immunol. 2014;104:Unit 15–25.
13. Eichele DD, Kharbanda KK. Dextran sodium sulfate colitis murine model: an indispensable tool for advancing our understanding of inflammatory bowel diseases pathogenesis. World J Gastroenterol. 2017;23:6016–29.
14. Basri AM, Taha H, Ahmad N. A review on the pharmacological activities and phytochemicals of *Alpinia officinarum* (Galangal) extracts derived from bioassay-guided fractionation and isolation. Pharmacogn Rev. 2017;11:43–56.
15. Lee C-C, Lin M-L, Meng M, Chen S-S. Galangin induces p53-independent S-phase arrest and apoptosis in human nasopharyngeal carcinoma cells through inhibiting PI3 K–AKT signaling pathway. Anticancer Res. 2018;38:1377–89.
16. Kumar R, Tiku A. Galangin induces cell death by modulating the expression of glyoxalase-1 and Nrf-2 in HeLa cells. Chem Biol Interact. 2018;279:1–9.
17. Jung YC, Kim ME, Yoon JH, Park PR, Youn H-Y, Lee H-W, et al. Anti-inflammatory effects of galangin on lipopolysaccharide-activated macrophages via ERK and NF-κB pathway regulation. Immunopharmacol Immunotoxicol. 2014;36:426–32.
18. Kale VM, Namdeo AG. Antiarthritic effect of galangin isolated from rhizomes of *Alpinia officinarum* in complete Freund's adjuvant-induced arthritis in rats. Int J Pharm Pharm Sci. 2014;6:499–505.
19. Jung CH, Jang SJ, Ahn J, Gwon SY, Jeon TI, Kim TW, et al. Alpinia officinarum inhibits adipocyte differentiation and high-fat diet-induced obesity in mice through regulation of adipogenesis and lipogenesis. J Med Food. 2012;15:959–67.
20. Aloud AA, Veeramani C, Govindasamy C, Alsaif MA, El Newehy AS, Al-Numair KS. Galangin, a dietary flavonoid, improves antioxidant status and reduces hyperglycemia-mediated oxidative stress in streptozotocin-induced diabetic rats. Redox Rep. 2017;22:290–300.
21. Tsai MS, Chien CC, Lin TH, Liu CC, Liu RH, Su HL, et al. Galangin prevents acute hepatorenal toxicity in novel propacetamol-induced acetaminophen-overdosed mice. J Med Food. 2015;18:1187–97.
22. Huang YC, Tsai MS, Hsieh PC, Shih JH, Wang TS, Wang YC, et al. Galangin ameliorates cisplatin-induced nephrotoxicity by attenuating oxidative stress, inflammation and cell death in mice through inhibition of ERK and NF-kappaB signaling. Toxicol Appl Pharmacol. 2017;329:128–39.
23. Tomar A, Vasisth S, Khan SI, Malik S, Nag TC, Arya DS, et al. Galangin ameliorates cisplatin induced nephrotoxicity in vivo by modulation of oxidative stress, apoptosis and inflammation through interplay of MAPK signaling cascade. Phytomedicine. 2017;34:154–61.
24. Shu YS, Tao W, Miao QB, Lu SC, Zhu YB. Galangin dampens mice lipopolysaccharide-induced acute lung injury. Inflammation. 2014;37:1661–8.
25. Huh JE, Jung IT, Choi J, Baek YH, Lee JD, Park DS, et al. The natural flavonoid galangin inhibits osteoclastic bone destruction and osteoclastogenesis by suppressing NF-kappaB in collagen-induced arthritis and bone marrow-derived macrophages. Eur J Pharmacol. 2013;698:57–66.
26. Sun S, Zhang H, Xue B, Wu Y, Wang J, Yin Z, et al. Protective effect of glutathione against lipopolysaccharide-induced inflammation and mortality in rats. Inflamm Res. 2006;55:504–10.
27. Sivakumar AS, Anuradha CV. Effect of galangin supplementation on oxidative damage and inflammatory changes in fructose-fed rat liver. Chem Biol Interact. 2011;193:141–8.
28. Luo Q, Zhu L, Ding J, Zhuang X, Xu L, Chen F. Protective effect of galangin in Concanavalin A-induced hepatitis in mice. Drug Des Devel Ther. 2015;9:2983–92.
29. Sahu BD, Kumar JM, Sistla R. Fisetin, a dietary flavonoid, ameliorates experimental colitis in mice: relevance of NF-kappaB signaling. J Nutr Biochem. 2016;28:171–82.
30. Sahu BD, Tatireddy S, Koneru M, Borkar RM, Kumar JM, Kuncha M, et al. Naringin ameliorates gentamicin-induced nephrotoxicity and associated mitochondrial dysfunction, apoptosis

and inflammation in rats: possible mechanism of nephroprotection. Toxicol Appl Pharmacol. 2014;277:8–20.
31. Lee HN, Shin SA, Choo GS, Kim HJ, Park YS, Kim BS, et al. Antiinflammatory effect of quercetin and galangin in LPS-stimulated RAW264.7 macrophages and DNCB-induced atopic dermatitis animal models. Int J Mol Med. 2018;41:888–98.
32. Zha WJ, Qian Y, Shen Y, Du Q, Chen FF, Wu ZZ, et al. Galangin abrogates ovalbumin-induced airway inflammation via negative regulation of NF-kappaB. Evid Based Complement Alternat Med. 2013;2013:767689.
33. Choi MJ, Lee EJ, Park JS, Kim SN, Park EM, Kim HS. Anti-inflammatory mechanism of galangin in lipopolysaccharide-stimulated microglia: critical role of PPAR-gamma signaling pathway. Biochem Pharmacol. 2017;144:120–31.
34. Choi MJ, Park JS, Park JE, Kim HS. Galangin suppresses pro-inflammatory gene expression in polyinosinic-polycytidylic acid-stimulated microglial cells. Biomol Ther (Seoul). 2017;25:641–7.
35. Ahmed SM, Luo L, Namani A, Wang XJ, Tang X. Nrf2 signaling pathway: pivotal roles in inflammation. Biochim Biophys Acta Mol Basis Dis. 2017;1863:585–97.
36. Singh R, Chandrashekharappa S, Bodduluri SR, Baby BV, Hegde B, Kotla NG, et al. Enhancement of the gut barrier integrity by a microbial metabolite through the Nrf2 pathway. Nat Commun. 2019;10:89.
37. Shen G, Kong AN. Nrf2 plays an important role in coordinated regulation of Phase II drug metabolism enzymes and Phase III drug transporters. Biopharm Drug Dispos. 2009;30:345–55.
38. Kobayashi EH, Suzuki T, Funayama R, Nagashima T, Hayashi M, Sekine H, et al. Nrf2 suppresses macrophage inflammatory response by blocking proinflammatory cytokine transcription. Nat Commun. 2016;7:11624.
39. Madduma Hewage SRK, Piao MJ, Kang KA, Ryu YS, Fernando P, Oh MC, et al. Galangin activates the ERK/AKT-driven Nrf2 signaling pathway to increase the level of reduced glutathione in human keratinocytes. Biomol Ther (Seoul). 2017;25:427–33.
40. Kim JK, Jang HD. Nrf2-mediated HO-1 induction coupled with the ERK signaling pathway contributes to indirect antioxidant capacity of caffeic acid phenethyl ester in HepG2 cells. Int J Mol Sci. 2014;15:12149–65.
41. Wardyn JD, Ponsford AH, Sanderson CM. Dissecting molecular cross-talk between Nrf2 and NF-kappaB response pathways. Biochem Soc Trans. 2015;43:621–6.
42. Khor TO, Huang MT, Kwon KH, Chan JY, Reddy BS, Kong AN. Nrf2-deficient mice have an increased susceptibility to dextran sulfate sodium-induced colitis. Cancer Res. 2006;66:11580–4.
43. Sanchez-Munoz F, Dominguez-Lopez A, Yamamoto-Furusho JK. Role of cytokines in inflammatory bowel disease. World J Gastroenterol. 2008;14:4280–8.
44. Strober W, Fuss IJ. Proinflammatory cytokines in the pathogenesis of inflammatory bowel diseases. Gastroenterology. 2011;140:1756–67.
45. Singer II, Kawka DW, Schloemann S, Tessner T, Riehl T, Stenson WF. Cyclooxygenase 2 is induced in colonic epithelial cells in inflammatory bowel disease. Gastroenterology. 1998;115:297–306.
46. Wang D, Dubois RN. The role of COX-2 in intestinal inflammation and colorectal cancer. Oncogene. 2010;29:781–8.